

UC San Diego

UC San Diego Previously Published Works

Title

Thermally Induced Silane Dehydrocoupling on Silicon Nanostructures

Permalink

<https://escholarship.org/uc/item/7rn28537>

Journal

Angewandte Chemie International Edition, 55(22)

ISSN

1433-7851

Authors

Kim, Dokyoung

Joo, Jinmyoung

Pan, Youlin

et al.

Publication Date

2016-05-23

DOI

10.1002/anie.201601010

Peer reviewed

Surface Modification

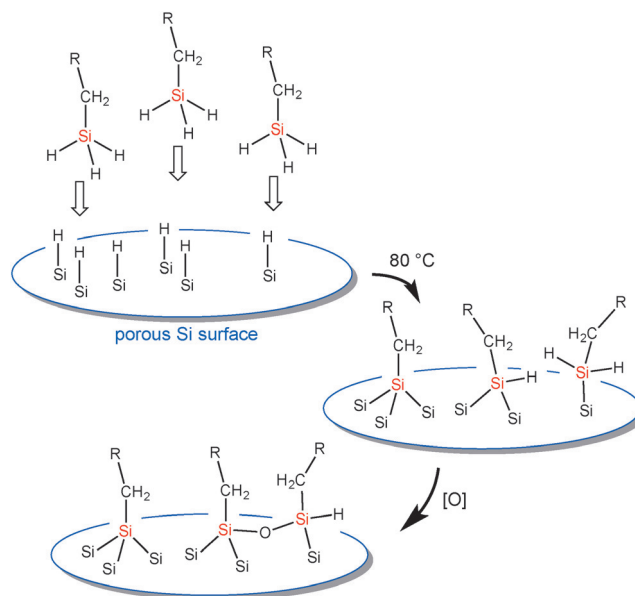
International Edition: DOI: 10.1002/anie.201601010
German Edition: DOI: 10.1002/ange.201601010

Thermally Induced Silane Dehydrocoupling on Silicon Nanostructures

Dokyoung Kim[†], Jinmyoung Joo[†], Youlin Pan, Alice Boarino, Yong Woong Jun, Kyo Han Ahn, Barry Arkles,^{*} and Michael J. Sailor^{*}

Abstract: Organic trihydridosilanes can be grafted to hydrogen-terminated porous Si nanostructures with no catalyst. The reaction proceeds efficiently at 80 °C, and it shows little sensitivity to air or water impurities. The modified surfaces are stable to corrosive aqueous solutions and common organic solvents. Octadecylsilane $H_3Si(CH_2)_{17}CH_3$, and functional silanes $H_3Si(CH_2)_{11}Br$, $H_3Si(CH_2)_9CH=CH_2$, and $H_3Si(CH_2)_2-(CF_2)_5CF_3$ are readily grafted. When performed on a mesoporous Si wafer, the perfluoro reagent yields a superhydrophobic surface (contact angle 151°). The bromo-derivative is converted to azide, amine, or alkyne functional surfaces via standard transformations, and the utility of the method is demonstrated by loading of the antibiotic ciprofloxacin (35 % by mass). When intrinsically photoluminescent porous Si films or nanoparticles are used, photoluminescence is retained in the grafted products, indicating that the chemistry does not introduce substantial nonradiative surface traps.

Extensive effort has been expended on stabilizing the surface of silicon to improve its suitability for various energy, electronics, sensor, and biological applications.^[1] The hydrosilylation reaction developed by Buriak, Boukherroub, and many others has been a mainstay in the field because of the ease with which functional species can be incorporated into the surface and the relatively low hydrolytic reactivity of the resulting Si–C bonds.^[2] The hydrosilylation reaction involves coupling of surface Si–H species to alkene or alkyne moieties on the organic reagent, and it requires scrupulous exclusion of air and water to avoid oxidative side



Scheme 1. Proposed dehydrogenative coupling reactions between trihydridosilanes and hydrogenated silicon in the presence of air.

reactions with Si–H.^[2a] An alternative to hydrosilylation is dehydrogenative coupling, where a hydridosilane ($RSiH_3$) instead of an alkene ($RCH=CH_2$) is coupled to the surface Si–H species (Scheme 1). An advantage of this approach is that the high reactivity of the silane reagent with trace oxygen and water can be expected to reduce the possibility of oxidative side reactions with the Si–H surface. Buriak and co-workers reported the first grafting reaction of hydridosilanes with porous Si surfaces using early transition metal catalysts to effect the transformation.^[3] The presence of these highly reactive catalysts led to oxidative side reactions, and the utility of the method was not fully realized. More recently, Veinot and co-workers demonstrated coupling of organosilanes to hydrogen-terminated Si nanoparticles catalyzed by the rhodium complex known as Wilkinson's catalyst.^[4] Following on the report of non-catalyzed dehydrogenative coupling of organosilanes to various surfaces including silicon,^[5] in this work we find that the reaction proceeds under mild thermal conditions on pSi surfaces without any added catalyst to generate stable, functional coatings, with minimal oxidation, and with retention of the electronic quality of the original Si–H surface.

The silicon nanostructures used in this work were prepared in the form of porous Si (pSi) films or nanoparticles by electrochemical etching of silicon wafers in aqueous ethanolic HF (see Supporting Information for detailed experimental conditions). The electrochemical etch gener-

[*] Dr. D. Kim,^[†] Dr. J. Joo,^[†] A. Boarino, Prof. Dr. M. J. Sailor
Department of Chemistry and Biochemistry
University of California, San Diego
9500 Gilman Drive, La Jolla, CA 92093 (USA)
E-mail: msailor@ucsd.edu

Dr. Y. Pan, Dr. B. Arkles
Gelest Inc.
11 East Steel Rd., Morrisville, PA 19067 (USA)

Y. W. Jun, Prof. Dr. K. H. Ahn
Department of Chemistry
Pohang University of Science and Technology (POSTECH)
77 Cheongam-Ro, Nam-Gu, Pohang 790-784 (Rep. of Korea)

[†] These authors contributed equally to this work.

Supporting information and the ORCID identification number(s) for the author(s) of this article can be found under <http://dx.doi.org/10.1002/anie.201601010>.

© 2016 The Authors. Published by Wiley-VCH Verlag GmbH & Co. KGaA. This is an open access article under the terms of the Creative Commons Attribution Non-Commercial NoDerivs License, which permits use and distribution in any medium, provided the original work is properly cited, the use is non-commercial, and no modifications or adaptations are made.

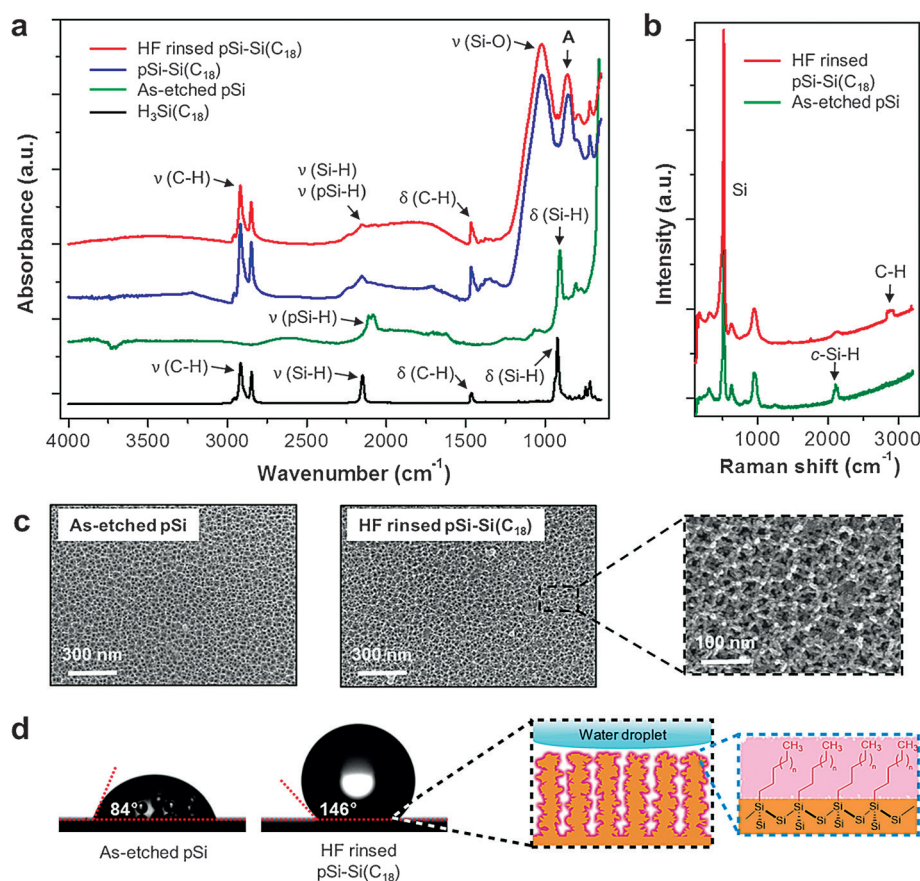


Figure 1. Characterization of coupling product of porous Si with octadecylsilane, $\text{H}_3\text{Si}(\text{C}_{18})$. a) Attenuated total reflectance Fourier-transform infrared (ATR-FTIR) spectra of the reactants and products. From bottom to top: neat octadecylsilane reagent (black trace); as-etched pSi starting material (green trace); porous Si with grafted octadecylsilane (blue trace); same grafted pSi sample, after thorough rinsing with aqueous ethanolic HF (red trace). Assignments of Si–H and C–H stretching and C–H bending (scissor) and Si–H deformation modes are indicated. Symbols: ν = stretching, δ = bending. Si = peaks associated with organosilane reagent, pSi = peaks associated with porous silicon substrate. b) Raman spectra obtained before (lower, green trace) and after (upper, red trace) grafting reaction. c) Plan view scanning electron microscope (SEM) images of sample before (upper) and after (lower) grafting reaction. Apparent median pore size is 20 nm. Grafted sample was rinsed with ethanolic aqueous HF after the grafting reaction. d) Water contact angle image and illustration of the surface. Contact angle values $\pm 5^\circ$, average of 5 individual sets. Initial porosity of all pSi samples 50–60%.

ated a mesoporous silicon skeleton terminated on the surface with hydrogen atoms. We first investigated the reaction of a pSi film with octadecylsilane, $\text{H}_3\text{Si}(\text{CH}_2)_{17}\text{CH}_3$ (“ $\text{H}_3\text{Si}(\text{C}_{18})$ ”). After heating to 80°C in the presence of the neat silane reagent and workup involving thorough rinsing of the sample (Figure S1 in the Supporting Information), infrared, Raman, and contact angle measurements (Figure 1) were indicative of extensive surface grafting. The modified porous layer (pSi–Si(C_{18})) was significantly more hydrophobic than either the pSi starting material or the non-porous Si substrate (Figure 1d and Figure S2), and the infrared spectrum of the product (Figure 1a) displayed bands associated with the organosilane, and additional strong bands at 1020 cm^{-1} and 860 cm^{-1} . By analogy with prior literature on organosilanes and modified silicon surfaces, the 1020 cm^{-1} band is assigned primarily to Si–O stretching $\nu(\text{Si}-\text{O})$, while the 860 cm^{-1} band (labeled A in Figure 1a) is assigned to modes associated

with the Si–C grafted aliphatic. For example, the C–Si–H bend in sila-cyclohexane^[6] appears as a strong band at 865 cm^{-1} , and the SiH₂ wag in diethylsilane^[7] appears as a very strong band at 840 cm^{-1} . A sharp band appeared in the spectrum of the as-prepared pSi starting material at 907 cm^{-1} , assigned to the SiH₂ scissor mode $\delta(\text{pSi}-\text{H})$, and in the octadecylsilane starting material the corresponding SiH₃ deformation mode^[8] $\delta(\text{Si}-\text{H})$ appeared at 922 cm^{-1} .

The Raman spectrum of pSi–Si(C_{18}) (Figure 1b) showed that the crystallinity of the material was retained (Si lattice mode at 515 cm^{-1}), and scanning electron microscope (SEM) images (Figure 1c) demonstrated that the open pore structure was preserved. Optical porosity measurements indicated that the grafting reaction decreased the open porosity of the pSi samples somewhat (Figure S3 and Table S1).

Because oxidation of pSi (to pSiO₂) involves a large volume expansion in the pore walls, oxidizing conditions can close the pores and trap material such that it cannot be readily washed out.^[9] Thus we performed tests to determine if the organosilane was chemically bonded to the pSi surface, rather than merely physically trapped in the pores. Thorough rinsing of the samples in an aqueous solution of HF-containing ethanol has become a standard test to determine if a species is grafted via Si–C

bonds, because HF attacks and dissolves Si–O bonds much more rapidly than Si–Si or Si–C bonds.^[1c,2a] Treatment of the octadecylsilane-grafted pSi product with aqueous ethanolic HF resulted in no change in the FTIR features associated with the surface modification (Figure 1a) and elemental analysis by energy-dispersive X-ray (EDS) analysis revealed strong carbon and oxygen signals (Table S2). By contrast, a control sample consisting of thermally oxidized pSi subjected to the same dehydrogenative coupling conditions and then treated with HF resulted in complete removal of the FTIR signatures of the octadecylsilane reagent (Figure S4). Therefore we conclude that the grafting reaction on hydrogen-terminated pSi results in organosilane covalently bonded to the pSi surface. The silicon oxide observed in the FTIR and EDS measurements is presumably beneath this grafted layer, formed by adventitious oxidation during the grafting reaction (Scheme 1). The grafted organosilane has sufficiently high

coverage that it protects this sub-surface oxide from attack by aqueous ethanolic HF.

Based on infrared and contact angle measurements, the optimal temperature to form pSi-Si(C₁₈) was determined to be 80 °C (Figure S5a). This temperature is substantially lower than the >100 °C temperatures typically employed when thermal hydrosilylation is used to attach alkenes to pSi surfaces,^[2a,10] and it minimizes side-reactions that can occur in the presence of adventitious oxygen or water. Control experiments performed in the absence of silane reagent indicated little oxidation of the pSi substrate at 80 °C, while at 120 °C, pSi surface oxidation was more substantial (Figure S5b). An additional control reaction determined that octadecylsilane did not react in the absence of pSi under the reaction conditions (80 °C, 24 h), i.e., the reagent does not undergo a dehydrogenative coupling reaction with itself (by NMR, Figure S6). The optimal reaction time for the reaction at 80 °C was determined to be 24 h, though surface grafting was apparent after 1 h (Figure S7). Based on contact angle and infrared measurements, the degree of surface coverage was readily tunable by adjustment of the reaction time between 1–24 h.

The dehydrocoupling reaction is remarkably tolerant of water and air; the reaction was found to proceed as well in air as in argon ambient, and introduction of up to 10% (by volume) water to the reaction mixture did not adversely affect the grafting reaction (Figure S8), although formation of silicon oxide as a side-product was observed by FTIR in all the reactions. As expected for a Si–C modified surface,^[2a,11] the organosilane-grafted pSi-Si(C₁₈) product displayed substantial stability toward harsh conditions such as heat (120 °C), light (224 mW cm⁻²), or strongly oxidative (1M H₂O₂) or acidic (1M HCl) conditions (Figure S9).

The dehydrocoupling reaction was also found to proceed on pSi nanoparticles. Porous silicon nanoparticles (pSiNPs) were prepared by ultrasonic fracture of a free-standing pSi film as previously described,^[12] except that the ultrasonication step was performed with the film immersed in neat hydrosilane reagent. This directly generated a homogeneous distribution of hydrophobic particles of average hydrodynamic size 160 nm (Figure S10). For either the pSi film or pSi nanoparticle grafting reactions, we believe the probable mechanism to be a combination of dehydrogenative coupling and dissociative adsorption on the strained hydrogenated silicon surface as indicated in

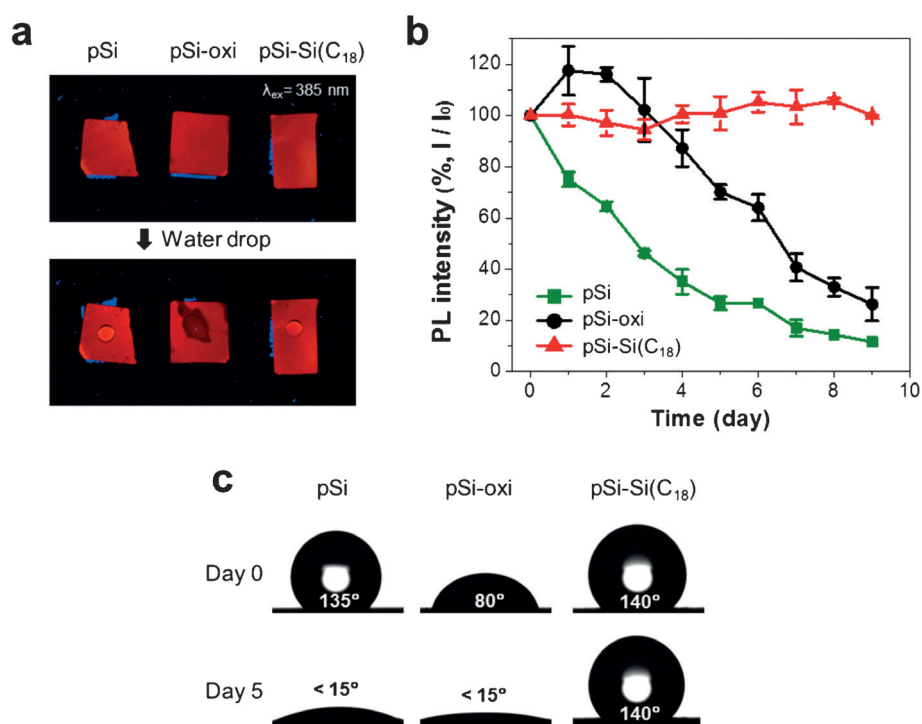


Figure 2. Dehydrocoupling reaction preserves the intrinsic photoluminescence of pSi. a) Photoluminescence (PL) images ($\lambda_{ex} = 385 \text{ nm}$) of as-etched pSi (pSi), thermally oxidized pSi (pSi-oxi), and coupling product pSi-Si(CH₂)₁₇CH₃ (pSi-Si(C₁₈)). All display room-temperature PL. The pSi and pSi-Si(C₁₈) samples are hydrophobic and added water does not wet the surface. The pSi-oxi sample (thermally oxidized at 80 °C for 24 h) is hydrophilic and PL is quenched by water. b) The integrated PL intensity ($\lambda_{em} = 500\text{--}950 \text{ nm}$) from the indicated samples as a function of time submerged in water. Samples were removed from water and dried prior to each measurement. c) Water contact angle of each sample, as indicated, at day 0 and day 5. Water contact angle standard error is $\pm 5^\circ$ from 3 replicate measurements.

Scheme 1, although detailed mechanistic studies were not performed.

To test the effect of the surface grafting reaction on the intrinsic photoluminescence of quantum-confined pSi,^[13] we prepared luminescent pSi from n-type silicon wafers. The n-type preparation displays strong photoluminescence (PL) immediately after electrochemical etching (Figure 2a and Figure S11).^[1c] Chemical reactions with this type of surface often lead to loss of photoluminescence due to the generation of non-radiative carrier traps.^[14] However, some reactions—in particular oxidation^[15] and hydrocarbon grafting^[2b,16]—have been found to passivate the surface and preserve photoluminescence from pSi. Similar to these surface-passivating reactions, the octadecylsilane dehydrocoupling reaction was found to preserve photoluminescence (Figure 2 and Figure S11). The pSi-Si(C₁₈) coupling product displayed a strongly hydrophobic character similar to the hydride-terminated pSi starting material. However, consistent with prior observations,^[17] hydride-terminated pSi slowly lost photoluminescence intensity and became more hydrophilic when submerged in water (Figure 2). Thermally oxidized (Si–SiO₂ core–shell) pSi samples displayed similar degradation of photoluminescence. This behavior results from oxidation and dissolution of the quantum-confined silicon nanostructures in the sample.^[17] By contrast, the coupling product pSi-Si(C₁₈) retained its photoluminescence and large contact angle

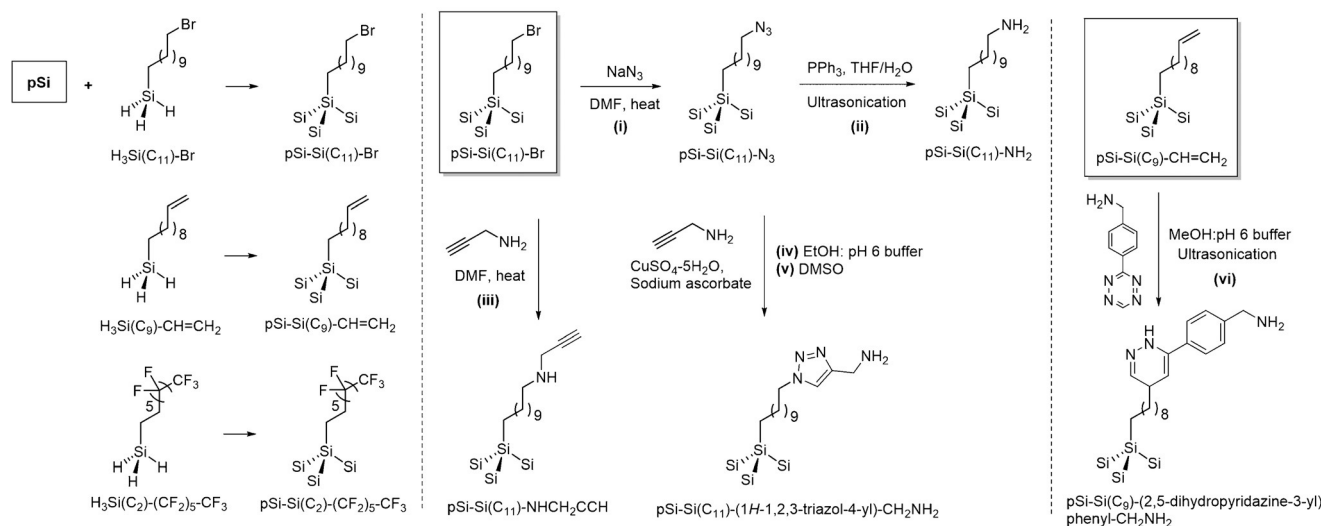


Figure 3. Summary of the reactions of functional hydrosilanes with pSi, and subsequent modification chemistry performed on the products. The coupling reactions of pSi chips with the functional hydrosilane reagents $\text{H}_3\text{Si}(\text{CH}_2)_{11}\text{Br}$, $\text{H}_3\text{Si}(\text{CH}_2)_9\text{CH}=\text{CH}_2$, and $\text{H}_3\text{Si}(\text{CH}_2)_2(\text{CF}_2)_5\text{CF}_3$ generate the grafted products pSi-Si(C_{11})-Br, pSi-Si(C_9)-CH=CH $_2$, and pSi-Si(C_2)-(CF $_2$) $_5$ CF $_3$, respectively (left side). The chips containing the products pSi-Si(C_{11})-Br and pSi-Si(C_9)-CH=CH $_2$ were subjected to subsequent chemical reactions: i) Reaction of pSi-Si(C_{11})-Br with NaN_3 generates pSi-Si(C_{11})-N $_3$. ii) Ultrasonic irradiation of pSi-Si(C_{11})-N $_3$ with PPh_3 in tetrahydrofuran yields pSi-Si(C_{11})-NH $_2$ (Staudinger reaction). iii) Reaction of pSi-Si(C_{11})-Br with propargylamine under basic conditions yields pSi-Si(C_{11})-NHCH $_2$ CCH. iv) Reaction of pSi-Si(C_{11})-N $_3$ with propargylamine in the presence of catalytic Cu^{2+} and sodium ascorbate generates pSi-Si(C_{11})-(1H-1,2,3-triazol-4-yl)-CH $_2$ NH $_2$ (catalyzed “click” reaction) in either aqueous (iv) or dimethylsulfoxide (v) solvents. vi) Ultrasonic irradiation of pSi-Si(C_9)-CH=CH $_2$ with (4-(1,2,4,5-Tetrazin-3-yl)phenyl) methanamine hydrochloride yields pSi-Si(C_9)-6-phenyl-1,4-dihydropyridazine-CH $_2$ NH $_2$ (uncatalyzed “click” reaction).

(> 140°) even after 9 days of immersion in aerated water. This behavior is similar to the behavior of luminescent pSi after it has been grafted with alkyl species by hydrosilylation.^[2a,18] However, as with p-type pSi, the dehydrocoupling reaction on n-type pSi showed substantially superior tolerance to air and water impurities compared with the hydrosilylation reaction (Figure S12).

Although the chemical stability imparted by Si-C-grafted organic species on pSi surfaces is required for many applications, perhaps the most important feature of grafting reactions is their ability to yield functional surfaces.^[2c] We found the organosilane dehydrocoupling reaction to be tolerant of functional groups and demonstrated several key functionalization reactions on pSi surfaces, summarized in Figure 3. In particular, functional hydrosilanes containing bromo and alkene terminal groups were successfully grafted, and the strongly hydrophobic perfluorocarbon hydrosilane was also grafted. The functional groups on the silane reagent retained their integrity, and the perfluorocarbon product displayed superhydrophobic behavior, with a water contact angle of 150° (Figure S13 and S14). As with the octadecylsilane derivative, these surface chemistries were not removed with aggressive rinsing in organic solvent or in aqueous ethanolic HF (Figure S15), establishing the Si-Si and Si-C bonding motif of the surface grafting reaction.

To test its suitability for further organic functionalization reactions, the pSi-Si(C_{11})-Br derivative was subjected to various common temperature-time-solvent combinations (dimethyl formamide, dimethyl sulfoxide, dichloromethane, and tetrahydrofuran) and it demonstrated high durability (Figure S16). The substitution reaction of pSi-Si(C_{11})-Br with

sodium azide (NaN_3) proceeded smoothly (reaction (i) in Figure 3 and Figure S17), and the reaction product pSi-Si(C_{11})-N $_3$ readily underwent the Staudinger reaction^[19] with triphenylphosphine (PPh_3) to generate a terminal amine, pSi-Si(C_{11})-NH $_2$ (reaction (ii) in Figure 3 and Figure S17). This primary amine-terminal product is a useful starting point for many bioconjugation reactions,^[20] and it also provides a hydrophilic surface that is positively charged at physiologic pH, which enables electrostatic loading of various negatively charged drugs. As an exemplar of this latter feature, we loaded the antibiotic drug ciprofloxacin^[21] by electrostatic means into the amine-functionalized surface. Up to 35 ± 3 % by mass of the drug could be loaded into the porous matrix at pH 7 (Figure S18).

To demonstrate the ability to functionalize the pSi-Si(C_{11})-NH $_2$ derivative by chemical bond formation, the material was reacted with fluorescein isothiocyanate (FITC), which resulted in conjugation of the fluorescent molecule to the surface via an amide bond. After workup, the sample displayed the bright green fluorescence spectrum characteristic of fluorescein, and infrared measurements confirmed the integrity of the attachment chemistry (Figure S19). The water contact angle increased substantially upon fluorescein conjugation, indicative of replacement of the highly hydrophilic amine species (contact angle 16°) with the more hydrophobic fluorescein molecule (contact angle 72°).

The bromo derivative pSi-Si(C_{11})-Br underwent a nucleophilic substitution reaction with the amine of propargylamine (reaction (iii) in Figure 3 and Figure S20), while the azide on the pSi-Si(C_{11})-N $_3$ derivative reacted with the alkyne moiety

of propargylamine in a copper-catalyzed “click” reaction^[22] (reaction (iv) and (v) in Figure 3 and Figure S17). Because residual metals can be problematic for therapeutic applications of nanomaterials, we also demonstrated the catalyst-free “click” reaction: tetrazine(phenyl)methanamine hydrochloride with the pSi-Si(C₉)-CH=CH₂ derivative (reaction (vi) in Figure 3, Figure S21 and Figure S22). This tetrazine-alkene “click” reaction proceeds without added catalyst.^[23] These reactions all occurred under mild conditions, and they were characterized by infrared spectroscopy, water contact angle measurements, and optical absorbance.

In summary, dehydrogenative coupling of hydrido-organo-silanes (H₃SiR) provides a mild, efficient, and experimentally convenient means to attach Si–C bonded species to hydrogen-terminated Si surfaces. The method is tolerant of terminal -Br and -alkene substituents, allowing entry into a range of useful functional nanomaterials and nanoparticles. The chemistry proceeds via Si–Si bond formation, which yields chemically stable surface that preserve photoluminescence from quantum-confined Si domain in the porous Si matrix.

Acknowledgements

This work was supported by the National Science Foundation under Grant No. DMR-1210417 and by the Defense Advanced Research Projects Agency (DARPA) under Cooperative Agreement HR0011-13-2-0017. The content of the information within this document does not necessarily reflect the position or the policy of the Government. K.H.A. acknowledges support from S. Korean Grant No. GRL 2014K1A1A2064569.

Keywords: mesoporous materials · photoluminescence · porous silicon · quantum dots · surface chemistry

How to cite: *Angew. Chem. Int. Ed.* **2016**, *55*, 6423–6427
Angew. Chem. **2016**, *128*, 6533–6537

- [1] a) L. T. Canham, *Handbook of Porous Silicon*, Springer, **2014**; b) L. T. Canham in *Porous Silicon for Biomedical Applications* (Ed.: H. A. Santos), **2014**, pp. 3–20; c) M. J. Sailor, *Porous Silicon in Practice: Preparation, Characterization, and Applications*, Wiley-VCH, Weinheim, **2012**.
- [2] a) J. M. Buriak, *Chem. Rev.* **2002**, *102*, 1271–1308; b) R. Boukherroub, J. T. C. Wojtyk, D. D. M. Wayner, D. J. Lockwood, *J. Electrochem. Soc.* **2002**, *149*, H59–H63; c) S. Ciampi, J. B. Harper, J. J. Gooding, *Chem. Soc. Rev.* **2010**, *39*, 2158–2183; d) J. M. Buriak, *Chem. Mater.* **2014**, *26*, 763–772.
- [3] Y. H. Li, J. M. Buriak, *Inorg. Chem.* **2006**, *45*, 1096–1102.
- [4] Z. Yang, M. H. Wahl, J. G. C. Veinot, *Can. J. Chem.* **2014**, *92*, 951–957.
- [5] B. Arkles, Y. Pan, Y. M. Kim, E. Eisenbraun, C. Miller, A. E. Kaloyeros, *J. Adhes. Sci. Technol.* **2012**, *26*, 41–54.
- [6] G. A. Guirgis, C. J. Nielsen, A. Horn, V. Aleksa, P. Klæboe, *J. Mol. Struct.* **2012**, *1023*, 189–196.
- [7] H. Matsuura, K. Ohno, T. Sato, H. Murata, *J. Mol. Struct.* **1979**, *52*, 13–26.
- [8] H. D. Stidham, A. J. LaPlante, J.-J. Oh, D. A. Obenchain, S. A. Peebles, R. A. Peebles, C. J. Wurrey, E. Marrow, G. A. Guirgis, *J. Mol. Struct.* **2011**, *1003*, 31–40.
- [9] a) P. S. Chaudhari, A. Gokarna, M. Kulkarni, M. S. Karve, S. Bhoraskar, *Sens. Actuators B* **2005**, *107*, 258–263; b) N. L. Fry, G. R. Boss, M. J. Sailor, *Chem. Mater.* **2014**, *26*, 2758–2764.
- [10] J. M. Buriak, *Chem. Commun.* **1999**, 1051–1060.
- [11] a) M. R. Linford, C. E. D. Chidsey, *J. Am. Chem. Soc.* **1993**, *115*, 12631–12632; b) M. R. Linford, C. E. D. Chidsey, *Langmuir* **2002**, *18*, 6217–6221.
- [12] Z. Qin, J. Joo, L. Gu, M. J. Sailor, *Part. Part. Syst. Charact.* **2014**, *31*, 252–256.
- [13] a) L. T. Canham, *Appl. Phys. Lett.* **1990**, *57*, 1046–1048; b) A. G. Cullis, L. T. Canham, *Nature* **1991**, *353*, 335–338.
- [14] a) V. La Ferrara, G. Fiorentino, G. Rametta, G. Di Francia, *Phys. Status Solidi A* **2012**, *209*, 736–740; b) J. L. Coffey, *J. Lumin.* **1996**, *70*, 343–351; c) R. R. Chandler-Henderson, B. Sweryda-Krawiec, J. L. Coffey, *J. Phys. Chem.* **1995**, *99*, 8851–8855; d) D. Andsager, J. Hilliard, M. H. Nayfeh, *Appl. Phys. Lett.* **1994**, *64*, 1141–1143; e) J. M. Lauerhaas, M. J. Sailor, *Science* **1993**, *261*, 1567–1568.
- [15] a) V. Petrova-Koch, T. Muschik, A. Kux, B. K. Meyer, F. Koch, V. Lehmann, *Appl. Phys. Lett.* **1992**, *61*, 943–945; b) B. Gelloz, N. Koshida, *Thin Solid Films* **2006**, *508*, 406–409.
- [16] a) Z. F. Li, E. Ruskenstein, *Nano Lett.* **2004**, *4*, 1463–1467; b) C. Vieillard, M. Warntjes, F. Ozanam, J.-N. Chazalviel, in *Proc. Electrochem. Soc.*, Vol. 95–25 (Eds.: D. J. Lockwood, P. M. Fauchet, N. Koshida, S. R. J. Brueck), Chicago, **1996**, pp. 250–258; c) R. J. Clark, M. K. M. Dang, J. G. C. Veinot, *Langmuir* **2010**, *26*, 15657–15664; d) M. P. Stewart, J. M. Buriak, *J. Am. Chem. Soc.* **2001**, *123*, 7821–7830.
- [17] a) X. Y. Hou, G. Shi, W. Wang, F. L. Zhang, P. H. Hao, D. M. Huang, X. Wang, *Appl. Phys. Lett.* **1993**, *62*, 1097–1098; b) B. Gelloz, A. Loni, L. Canham, N. Koshida, *Nanoscale Res. Lett.* **2012**, *7*, 382; c) J. Joo, J. F. Cruz, S. Vijayakumar, J. Grondek, M. J. Sailor, *Adv. Funct. Mater.* **2014**, *24*, 5688–5694.
- [18] a) J. M. Buriak, M. J. Allen, *J. Am. Chem. Soc.* **1998**, *120*, 1339–1340; b) J. M. Buriak, M. J. Allen, *J. Lumin.* **1998**, *80*, 29–35.
- [19] H. Staudinger, J. Meyer, *Helv. Chim. Acta* **1919**, *2*, 635–646.
- [20] a) I. L. Medintz, H. T. Uyeda, E. R. Goldman, H. Mattoussi, *Nat. Mater.* **2005**, *4*, 435–446; b) G. T. Hermanson, *Bioconjugate Techniques*, Academic Press, San Diego, **1996**.
- [21] a) T. Guinan, C. Godefroy, N. Lautredou, S. Pace, P. E. Milhiet, N. Voelcker, F. Cunin, *Langmuir* **2013**, *29*, 10279–10286; b) N. Ehlert, M. Badar, A. Christel, S. J. Lohmeier, T. Luessenhop, M. Stieve, T. Lenarz, P. P. Mueller, P. Behrens, *J. Mater. Chem.* **2011**, *21*, 752–760.
- [22] J. E. Hein, V. V. Fokin, *Chem. Soc. Rev.* **2010**, *39*, 1302–1315.
- [23] a) J. C. Jewett, C. R. Bertozzi, *Chem. Soc. Rev.* **2010**, *39*, 1272–1279; b) A. Niederwieser, A. K. Spate, L. D. Nguyen, C. Jungst, W. Reutter, V. Wittmann, *Angew. Chem. Int. Ed.* **2013**, *52*, 4265–4268; *Angew. Chem.* **2013**, *125*, 4359–4363.

Received: January 28, 2016

Published online: April 21, 2016